

Bis(trimethylsilyl)benzamidinate zirconium dichlorides. Active catalysts for ethylene polymerization

Dorit Herskovics-Korine, Moris S. Eisen *

Department of Chemistry, Technion–Israel Institute of Technology, Haifa 32000, Israel

Received 6 March 1995

Abstract

A study was made of the polymerization of ethylene involving the use of a series of $[\eta^4\text{-}4\text{-RC}_6\text{H}_4\text{C(NSiMe}_3)_2]_2\text{ZrCl}_2$ as precatalysts ($\text{R} = \text{H}$ (**1**); CH_3 (**2**)). The benzamidinate zirconium dichloride complexes were prepared from ZrCl_4 and the corresponding $4\text{-RC}_6\text{H}_4\text{C(NSiMe}_3)_2\text{Li} \cdot \text{TMEDA}$ ligand. The structure of complex **1** was determined by a low-temperature X-ray diffraction study. "Cationic" ethylene polymerization catalysts were generated from **1** and **2** with methylalumoxane. The polymerization activity and the molecular weights of the polymers are strongly dependent on the catalyst and cocatalyst concentrations. The polymerization activity increases drastically with increase in pressure and temperature and decreases when electron-releasing groups are attached to the aromatic ring.

Keywords: Zirconium; Zirconocene; Ziegler–Natta polymerization; Benzamidinate; Crystal structure

1. Introduction

The study of ligand effects on the Ziegler–Natta polymerization of olefins using soluble Group 4 metallocene catalysts and methylaluminoxane cocatalyst has shed a great deal of light on the mechanism of this important process [1,2]. Much of the work in this area has been concerned with the way in which the catalytic activity and stereoregularities are influenced by steric hindrance at the metal centre [2]. Furthermore, some of the work has been directed toward the elucidation of the way in which the catalytic activity and molecular weights are influenced by changes in the electron density at the metal centre [3]. We were interested in examining zirconium-based systems with various metal coordination environments and comparing these with the known metallocene chemistry. We chose the previously employed bidentate *N,N'*-bis(trimethylsilyl)benzamidinate ligand to develop new catalytic Group IV chemistry for C–C and C–H bond formation [4]. Here we describe the preparation and characterization of bis[*N,N'*-bis(trimethylsilyl)benzamidinate]zirconium dichlorides **1** and **2**, $[\eta^4\text{-}4\text{-RC}_6\text{H}_4\text{C(NSiMe}_3)_2]_2\text{ZrCl}_2$ (R

$= \text{H}$ (**1**), CH_3 (**2**)) and their use as catalyst precursors for the polymerization of ethylene, and also report the X-ray solid state structure of **1**.

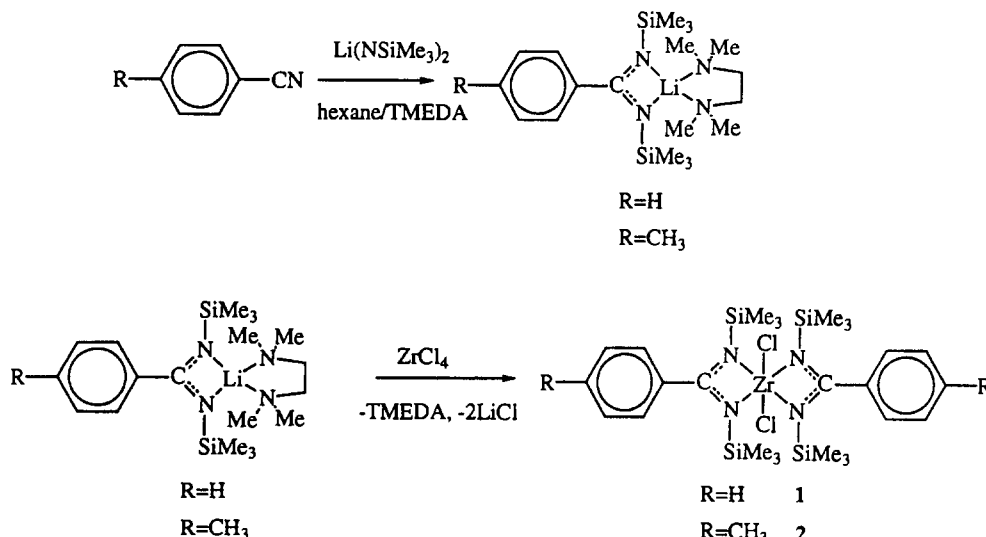
2. Results and discussion

2.1. Syntheses

The reaction of ZrCl_4 with 2 equiv. of the appropriate substituted bis(trimethylsilyl)benzamidinate lithium–TMEDA complex $4\text{-RC}_6\text{H}_4\text{C(NSiMe}_3)_2\text{Li} \cdot \text{TMEDA}$ (TMEDA = *N,N,N',N'*-tetramethylethylenediamine) ($\text{R} = \text{H}$, CH_3) took place at room temperature in toluene to give a pale yellow solution from which white rhombohedral crystals of **1** or **2** were isolated, after washing away the TMEDA, in good yield and analytically pure (Scheme 1).

Compounds **1** and **2** were also obtained, although in lower yields, by reaction of ZrCl_4 and 1 equiv. of the corresponding benzamidinate lithium dimer **3** or **4** (Scheme 2) [5]. When a diethyl ether–hexane solution of complex **1** was kept at -40°C , a 50–55% yield of the crystalline product was obtained and subjected to a low-temperature X-ray diffraction study. In spite of the fact that other zirconium-containing products are likely

* Corresponding author.



Scheme 1. Route to bis(benzamidinate) zirconium complexes.

to be formed, this reaction gives (probably by disproportionation) by far the best quality product in terms of crystallinity and purity.

2.2. Crystal structure of $[\text{C}_6\text{H}_5\text{C(NSiMe}_3)_2]_2\text{ZrCl}_2$ (**1**)

The crystallographic data for complex **1** are given in Tables 1, 3 and 4. The structure consists of a zirconium atom chelated by two benzamidinate ligands and connected to two chlorine atoms to give a distorted tetrahedral environment at the metal. The distorted tetrahedron is defined by centroids of the two benzamidinate ligands ($\text{C}(1)\text{-Zr}(1)\text{-C}(1)' = 124.8(3)^\circ$) and the two chlorine atoms ($\text{Cl}(1)\text{-Zr}(1)\text{-Cl}(1)' = 103.81(11)^\circ$). The two benzamidinate ligands form four-membered rings al-

most coplanar with the zirconium atom (torsion angle $\text{Zr}(1)\text{-N}(1)\text{-C}(1)\text{-N}(2) = 1.4^\circ$). The Zr-Cl distance ($2.401(2) \text{ \AA}$) and Zr-N distances [$\text{Zr}(1)\text{-N}(1) = 2.238(5)$, $\text{Zr}(1)\text{-N}(2) = 2.204(5) \text{ \AA}$] are significantly elongated with respect to the analogous titanium complex [6].

It is noteworthy that the two ancillary benzamidinate ligands lie in two non-symmetrical planes. The angles formed between the similar nitrogen atoms at each ligand change drastically from 170.6 to 90.3° ($\text{N}(1)\text{-Zr}(1)\text{-N}(1)' = 170.6(2)$, $\text{N}(2)\text{-Zr}(1)\text{-N}(2)' = 90.3(2)^\circ$) to form a $\text{Zr}(1)\text{-centroids}$ angle of $124.8(3)^\circ$. This angle, which is believed to be in part responsible for the catalytic activity (see below), is smaller than that (136°) in cyclopentadienyl complexes.

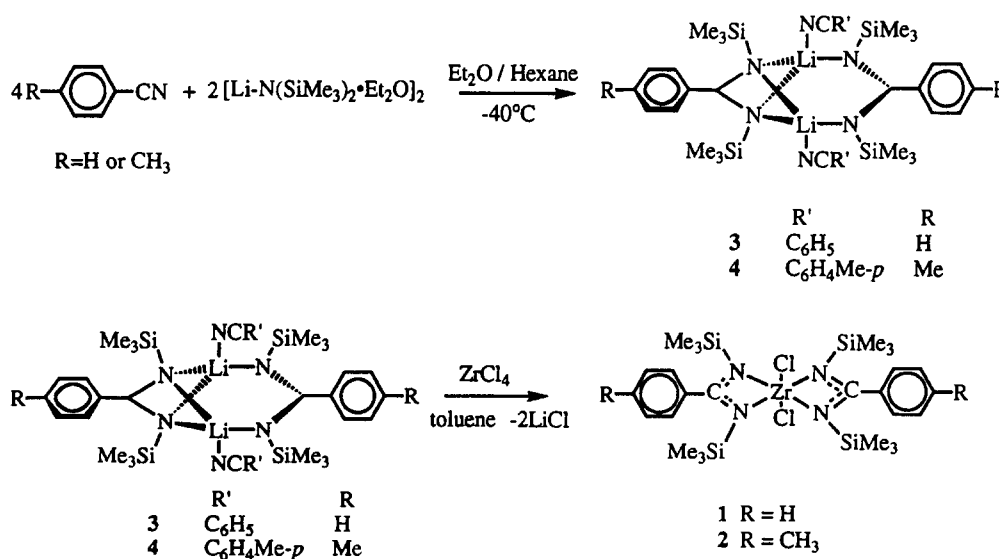
Scheme 2. Alternative route to complexes **1** and **2**.

Table 1
Bond lengths (Å) and angles (°) for complex **1**

Zr(1)–N(2)	2.204(5)	Si(2)–C(20)	1.859(6)
Zr(1)–N(1)	2.238(5)	Zr(1)–C(1)	2.636(5)
Zr(1)–Cl(1)	2.401(2)	N(1)–Si(1)	1.758(5)
N(1)–C(1)	1.338(7)	Si(1)–C(12)	1.844(7)
Si(1)–C(10)	1.843(6)	C(1)–N(2)	1.354(7)
Si(1)–C(11)	1.867(6)	C(100)–C(101)	1.394(8)
C(1)–C(100)	1.484(8)	C(101)–C(102)	1.374(8)
C(100)–C(105)	1.398(7)	C(103)–C(104)	1.394(9)
C(102)–C(103)	1.384(8)	N(2)–Si(2)	1.745(5)
C(104)–C(105)	1.377(8)	Si(2)–C(21)	1.858(6)
Si(2)–C(22)	1.857(6)		
N(2)–Zr(1)–N(2)#1	90.3(2)	N(2)–Si(2)–C(22)	105.3(2)
N(2)#1–Zr(1)–N(1)	111.4(2)	C(22)–Si(2)–C(20)	108.4(3)
N(2)–Zr(1)–N(1)	61.4(2)	C(22)–Si(2)–C(21)	108.7(3)
N(2)–Zr(1)–Cl(1)	91.01(12)	N(1)–Zr(1)–N(1)#1	170.6(2)
N(1)–Zr(1)–Cl(1)	96.77(13)	N(2)–Zr(1)–C(1)	30.9(2)
N(2)–Zr(1)–Cl(1)#1	148.48(12)	N(1)–Zr(1)–C(1)	30.5(2)
N(1)–Zr(1)–Cl(1)#1	89.01(12)	Cl(1)–Zr(1)–C(1)	92.25(12)
Cl(1)–Zr(1)–Cl(1)#1	103.81(11)	C(1)#1–Zr(1)–C(1)	124.8(3)
N(2)#1–Zr(1)–C(1)	101.8(2)	C(1)–N(1)–Zr(1)	91.4(3)
N(1)#1–Zr(1)–C(1)	141.8(2)	N(1)–Si(1)–C(10)	108.4(3)
Cl(1)#1–Zr(1)–C(1)	118.71(13)	C(10)–Si(1)–C(12)	110.0(3)
C(1)–N(1)–Si(1)	129.5(4)	C(10)–Si(1)–C(11)	110.5(3)
Si(1)–N(1)–Zr(1)	138.9(3)	N(1)–C(1)–N(2)	114.7(5)
N(1)–Si(1)–C(12)	109.0(3)	N(2)–C(1)–C(100)	121.9(5)
N(1)–Si(1)–C(11)	113.4(3)	N(2)–C(1)–Zr(1)	56.7(3)
C(12)–Si(1)–C(11)	105.4(3)	C(101)–C(100)–C(105)	118.7(5)
N(1)–C(1)–C(100)	123.4(5)	C(105)–C(100)–C(1)	121.3(5)
N(1)–C(1)–Zr(1)	58.1(3)	C(101)–C(102)–C(103)	120.8(6)
C(100)–C(1)–Zr(1)	177.8(4)	C(105)–C(104)–C(103)	119.9(5)
C(101)–C(100)–C(1)	120.0(5)	Si(2)–N(2)–Zr(1)	138.0(2)
C(102)–C(101)–C(100)	120.3(5)	N(2)–Si(2)–C(21)	113.7(3)
C(102)–C(103)–C(104)	119.4(6)	N(2)–Si(2)–C(20)	108.8(3)
C(104)–C(105)–C(100)	120.8(6)	C(21)–Si(2)–C(20)	111.6(3)
C(1)–N(2)–Zr(1)	92.5(3)		

A comparison of **1** with lanthanide/earlier transition metal complexes of the ligand reveals a small difference between the N(1)–C(1)–N(2) angle in **1**, 114.7(5)°, and those in analogous complexes of Nd, 121.4(5)° [7], in Ti(III), 116.5(2)° [8] in Y, 119.8(2)° [9], and Ti(IV), 112.9(3)° [6], and those of 122.5(6)° [10] and 115.0(5)° [11] in the mixed benzamidate–cyclopentadienyl Zr and Hf systems, respectively. This can be attributed to the slightly more ionic nature of the bonding character of the lanthanide and Ti(III) than with Ti(IV) and mixed cyclopentadienyl–benzamidate Zr(IV) systems. The opposite effect has been observed for *N*-phenyl-substituted amidinates with late transition metals [12]. An ORTEP drawing of the benzamidate zirconium dichloride complex is given in Fig. 1.

2.3. Polymerization activity studies

The catalytic polymerization of ethylene was studied using the catalyst precursors **1** and **2**. Cationic catalysts were generated by the reaction of the corresponding complexes with methylaluminoxane (MAO). The poly-

merizations were carried out under rigorously anaerobic/anhydrous vacuum line conditions, and reactions were quenched after appropriate times with methanol–HCl solutions prior to collection of the polymer, followed by washing with pentane and acetone and drying. The polymer microstructure of the high-density polyethylene obtained was characterized by ¹³C NMR spec-

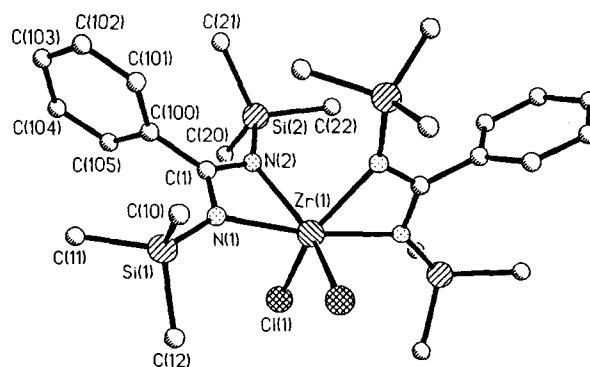


Fig. 1. The molecular structure of **1** showing the atom numbering scheme.

troscopy [13]. Molecular weights (M_n) were measured by the Ubbelohde calibrated viscosimeter technique and extrapolation to the intrinsic viscosity. Melting points were determined by DSC.

Several interesting trends are evident in the polymerization data (Table 2). The activity of the catalysts is strongly dependent on the temperature (entries 2–4). Thus, raising the temperature from 5 to 60°C causes an increase in catalytic activity by a factor of ca. 6. Large effects were observed for changes in the Al:Zr ratio (see entries 1, 3 and 5). An increase in the Al:Zr ratio results in a small decrease in catalytic activity but with retention of similar molecular weight and melting points for the polymers obtained. However, very interestingly, it can be seen that the smaller the MAO/catalyst ratio used the better the catalytic activity and the higher the molecular weight of the product. This behaviour is opposite to that observed with cyclopentadienyl early transition metal systems [1–3]. This result can be accounted for in terms of the known dependence on the cocatalyst concentration of the relative proportion of the various possible eliminations, alkyl transfer pathways and other deactivation processes [14]. Under otherwise similar conditions, high-pressure polymerization of ethylene (entry 7) involves the largest catalytic activity (by a factor of ca. 25) and gives polymers of higher molecular weight than at atmospheric pressure. We suggest that these effects are reasonably a consequence of the previously demonstrated tight, sterically demanding and varying ion pairing between the cationic reaction centre and the anionic methylalumoxane [2a,15]. In addition, the electronic effect of these benzamidinate ancillary ligands is clearly shown by comparing the catalyst precursors **1** and **2**. The latter contains a conjugatively electron-releasing group that causes a decrease in the electrophilicity of the metal and a concomitant decrease in the catalytic activity (entries 3 and 6).

It is very interesting to compare some of our results with those for similar catalytic polymerization systems containing the ancillary benzamidinate ligands. For ex-

ample, reactions of mixed cyclopentadienyl–benzamidinate titanium dichlorides and a large excess of MAO (Al/Ti = 839) have shown an ethylene catalytic activity of 0.6×10^5 g polymer (mol Ti)⁻¹ h⁻¹ atm⁻¹. The similar mixed system of zirconiumdimethyl with B(C₆F₅)₃ as cocatalyst has a smaller activity than TiMe₃, viz. 1.2×10^4 g polymer (mol Zr)⁻¹ h⁻¹ atm⁻¹, presumably owing to the side formation of the inert pentafluorophenyl complex [10,11]. The use of these hard basic benzamidinate ligands in place of both cyclopentadienyl groups stems from the fact that they are electron-withdrawing ancillary ligands and so should enhance the electrophilic character of the metal centre. The benzamidinate systems have four electron-donating groups with two coordination sites whereas the cyclopentadienyl ligand is six electron donating with three coordination sites. Comparison of the results for mixed systems (Zr, Ti) with those shown in Table 2 (entries 1 and 7) reveals that the presence of two benzamidinate ligands moderately improved the catalytic activity. It is important to point out that both systems have lower catalytic activity than the analogous cyclopentadienyl systems for the polymerization of ethylene (6×10^6 g (mol Zr)⁻¹ h⁻¹ atm⁻¹) [2a], despite the larger catalytic activity that was observed, for example, in the bis(benzamidinate)yttrium-catalysed oligomerization of alkynes [16].

The difference in catalytic activity between our ‘‘cationic’’ complexes and the cyclopentadienyl ‘‘cationic’’ systems can be understood in terms of the structural environment of the metal centre. Normally, it has been observed that the smaller the angle between the ancillary ligands, the more coordinatively unsaturated the metal centre of the complex is and the higher is the catalytic activity observed for the catalyst [17], although, in our case, we have a catalyst with lower reactivity for the catalytic polymerization of ethylene than the analogous cyclopentadienyl complexes. This activity–structure relationship for complex **1** can be simply illustrated by the fact that the small angle tilted

Table 2
Activity, molecular weight and melting point data for the polymerization of ethylene by bis(benzamidinate)zirconium complexes

Entry	Catalyst	T (°C)	[Cat] ^a	[Co-Cat] ^b	Mon ^c	Activity ^d	M_n ^e	M.p. (°C)
1	1	25	2.9×10^{-4}	0.057	1	3.2×10^4	150,000	133.9
2	1	5	2.9×10^{-4}	0.115	1	6.5×10^3	48,000	124.8
3	1	25	2.9×10^{-4}	0.115	1	2.6×10^4	49,950	129.6
4	1	60	2.9×10^{-4}	0.115	1	2.8×10^4	78,000	132.9
5	1	25	2.9×10^{-4}	0.230	1	2.4×10^4	50,570	133.4
6	2	25	2.9×10^{-4}	0.115	1	1.6×10^4	30,000	130.5
7	1	25	2.9×10^{-4}	0.115	5	5.7×10^5	162,000	135.4

^a [Catalyst], M in toluene.

^b [Co-catalyst], M in toluene, methylaluminoxane, solvent removed from a 20% solution in toluene (Schering) at 25°C/10⁻⁶ Torr.

^c [Monomer], pressure in atmospheres.

^d Grams total polymer (mol Zr)⁻¹ (atm ethylene)⁻¹ h⁻¹.

^e By viscosimeter technique in 1,2,4-trichlorobenzene at 130°C ($K = 5.96 \times 10^{-4}$; $a = 0.7$).

to the back of the molecule ($\text{N}(2)\text{--Zr}(1)\text{--N}(2)'$ = $90.3(2)^\circ$) will prevent the approach of the olefin from the back such as occurs in the cyclopentadienyl case, although the presence of the large angle $\text{N}(1)\text{--Zr}(1)\text{--N}(1)'$ = $170.6(2)^\circ$ with the two bulky equatorial SiMe_3 groups obstructs the approach from the side of the molecule, inducing the low catalytic activity (Fig. 2). This side approach is believed to be responsible for the catalytic polymerization activity of the metal centre which involves a four-centre transition state mechanism [18].

At present we are designing ancillary benzamidinate ligands such that the angles between the similar nitrogens in the different benzamidinate ligands will be equal or as close as possible.

3. Experimental section

All manipulations of air-sensitive materials were performed with the rigorous exclusion of oxygen and moisture in flamed Schlenk-type glassware on a dual-manifold Schlenk line, or interfaced to a high vacuum (10^{-5} Torr) line, or in a nitrogen-filled Vacuum Atmospheres glove-box with a medium-capacity recirculator (1–2 ppm O_2). Argon and nitrogen were purified by passage through a MnO oxygen-removal column and a Davison 4A molecular sieve column. Ether solvents were distilled under argon from sodium benzophenone ketyl. Hydrocarbon solvents (toluene- d_8 , C_6D_6 , hexane) and TMEDA were distilled under nitrogen from Na–K alloy. All solvents for vacuum line manipulations were stored in vacuum over Na–K alloy in resealable bulbs. Nitrile compounds (Aldrich) were degassed and freshly distilled under argon. $\text{LiN}(\text{TMS})_2$ (Aldrich), $\text{C}_6\text{H}_5\text{C}(\text{N-SiMe}_3)_2\text{Li} \cdot \text{TMEDA}$ [8], **3** [5] and **4** [5] were prepared according to the literature. NMR spectra were recorded on a Bruker AM 200 spectrometer. ^1H NMR chemical shifts are referenced to internal solvent resonances and are reported relative to tetramethylsilane. The NMR experiments were conducted in PTFE valve-sealed tubes

(J-Young) after vacuum transfer of the solvent in a high-vacuum line.

3.1. $4\text{-CH}_3\text{C}_6\text{H}_4\text{C}(\text{NSiMe}_3)_2\text{Li} \cdot \text{TMEDA}$

To 15.86 g (0.095 mol) of a well stirred suspension of $\text{LiN}(\text{TMS})_2$ in hexane (180 ml) at 0°C were added slowly 11.1 g (0.095 mol) of 4-methylbenzonitrile. The temperature was slowly raised to 50°C and the mixture was stirred for a further 3 h, then allowed to cool to room temperature. 14.48 g (0.123 mol) of TMEDA were added and the solution stirred for 1 hour. During the addition of the TMEDA, the solution turned brown-red and after several minutes a large amount of material separated out. The mixture was kept overnight at -50°C and then filtered while cold. The precipitate was dried under high vacuum to give 31.6 g (83%) of white crystals. ^1H NMR (200 MHz, C_6D_6): δ 7.07–7.04 (m, 4H, Ph), 2.43 (s, 4H, $\text{CH}_2\text{-N}$), 2.42 (s, 3H, CH_3), 2.27 (s, 12H, $\text{CH}_3\text{-N}$), -0.22 (s, 18H, $\text{CH}_3\text{-Si}$).

3.2. $[\eta^4\text{-C}_6\text{H}_5\text{C}(\text{NSiMe}_3)_2]_2\text{ZrCl}_2$ (**1**)

Into a glass vessel within a glove-box were weighed 1.66 g (7.12 mmol) of ZrCl_4 and 5.52 g (14.23 mmol) of $\text{C}_6\text{H}_5\text{C}(\text{NSiMe}_3)_2\text{Li} \cdot \text{TMEDA}$. Toluene (50 ml) was transferred into the vessel on the vacuum line and the solution was stirred for 24 h at room temperature. The LiCl was then filtered off through a C3 frit and the pale yellow filtrate was evaporated and the solid washed several times with diethyl ether–hexane to remove TMEDA. Yield 2.68 g (55%). Suitable crystals for the crystal structure determination were obtained by slow crystallization from a diethyl–hexane solution at -40°C . ^1H NMR (200 MHz, C_6D_6): δ 7.40–7.38 (m, 5H, Ph), -0.01 (s, 18H, $\text{CH}_3\text{-Si}$, 36H).

Owing to the extreme sensitivity of the compound towards moisture and oxygen, a suitable crystal for X-ray analysis was covered with Kel-F oil (Votalef) inside a glove-box and then mounted on the four-cycle

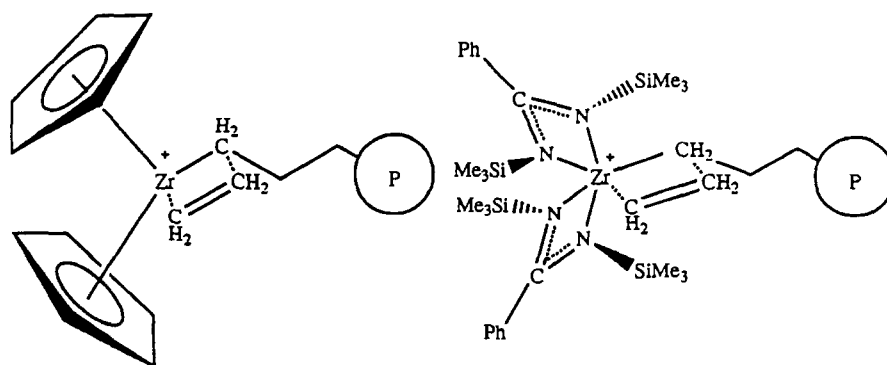


Fig. 2. Side view of the theoretical approach of ethylene in polymerization by zirconocene and benzamidinate zirconium cationic complexes.

Table 3

Crystal data, data collection and refinement for **1**

Empirical formula	C ₂₆ H ₄₆ Cl ₂ N ₄ Si ₄ Zr
Formula weight	689.15
Temperature (K)	173 (2)
Wavelength (Å)	0.71073
Crystal system	Monoclinic
Space group	C2/c
Unit cell dimensions:	
<i>a</i> (Å)	20.936(13)
<i>b</i> (Å)	9.267(6)
<i>c</i> (Å)	17.837(11)
β (°)	95.97(3)
Volume (Å ³)	3442(4)
Z	4
Density (calculated) (mg m ⁻³)	1.330
Absorption coefficient (mm ⁻¹)	0.636
<i>F</i> (000)	1440
Crystal size (mm)	0.6 × 0.2 × 0.1
θ range for data collection (°)	2.62 to 25.00
Index ranges:	
<i>h</i>	−24 → 24
<i>k</i>	−11 → 9
<i>l</i>	−1 → 21
Reflections collected	3655
Independent reflections	3002
<i>R</i> (int)	0.0449
Refinement method	Full-matrix least-squares on <i>F</i> ²
Data/restraints/parameters	3002/0/176
Goodness-of-fit on <i>F</i> ²	0.902
Final <i>R</i> indices:	
<i>R</i> ₁ (<i>I</i> > 2σ(<i>I</i>))	0.0583
<i>wR</i> ₂	0.1362
<i>R</i> indices (all data):	
<i>R</i> ₁	0.0914
<i>wR</i> ₂	0.1439
Largest difference peak (e Å ⁻³)	1.402
Largest difference hole (e Å ⁻³)	−1.593

Table 4

Atomic coordinates (×10⁴) and equivalent isotropic displacement parameters (Å² × 10³) for complex **1**

Atom	<i>x</i>	<i>y</i>	<i>z</i>	<i>U</i> _{eq} ^a
Zr(1)	0	3203(1)	2500	20(1)
Cl(1)	422(1)	4802(2)	1614(1)	49(1)
N(1)	902(2)	3006(5)	3285(2)	22(1)
Si(1)	1297(1)	3911(2)	4066(1)	27(1)
C(10)	980(4)	3232(9)	4926(3)	49(2)
C(11)	2189(3)	3722(8)	4142(4)	39(2)
C(12)	1141(3)	5863(7)	3964(4)	42(2)
C(1)	1099(2)	1885(6)	2896(3)	21(1)
C(100)	1705(2)	1090(6)	3114(3)	21(1)
C(101)	1745(3)	129(6)	3718(3)	26(1)
C(102)	2304(3)	−616(7)	3921(3)	33(2)
C(103)	2838(3)	−420(7)	3535(4)	33(2)
C(104)	2804(3)	535(7)	2929(4)	30(2)
C(105)	2243(3)	1271(6)	2719(3)	26(1)
N(2)	702(2)	1526(5)	2276(2)	21(1)
Si(2)	799(1)	226(2)	1589(1)	24(1)
C(20)	1253(3)	1040(8)	852(3)	39(2)
C(21)	1182(3)	−1465(6)	1971(3)	32(2)
C(22)	−26(3)	−196(7)	1159(3)	36(2)

^a *U*_{eq} is defined as one third of the trace of the orthogonalized *U*_{*ij*} tensor.

diffractometer where it was held in a cold stream of nitrogen at 173 K. Reflections were collected on a Siemens P4 automated four-cycle diffractometer. Intensities were corrected in the usual way except for absorption. The structure was solved by direct methods, and refined on F^2 by full matrix least-squares procedures. All non-hydrogen atoms were refined with anisotropic temperature coefficients. The hydrogen atoms were included by use of a riding model and refined isotropically, with $d(\text{C-H})$ 0.95 Å for the aromatic and 0.98 Å for the methyl hydrogens. Crystal data, measurement conditions and details of the structure refinement are shown in Table 3. Final atomic coordinates are given in Table 4. Additional material deposited at the Cambridge Crystallographic Data Centre includes thermal parameters and hydrogen coordinates.

3.3. $[\eta^4\text{-}4\text{-CH}_3\text{C}_6\text{H}_4\text{C}(\text{NSiMe}_3)_2\text{ZrCl}_2$ (2)

In a procedure similar to that used for **1**, 1.05 g (4.5 mmol) of ZrCl_4 was treated with 3.60 g (9.0 mmol) of $4\text{-CH}_3\text{C}_6\text{H}_4\text{C}(\text{NSiMe}_3)_2\text{Li} \cdot \text{TMEDA}$ to give 2.8 g (86%) of complex **2**. $\text{C}_{28}\text{H}_{50}\text{Cl}_2\text{N}_4\text{Si}_4\text{Zr}$, calc. C 46.93, H 6.98, N 7.82, Cl 9.91; found C 46.54, H 7.04, N 8.19, Cl 9.81%. $^1\text{H NMR}$ (200 MHz, C_6D_6): δ 7.18 (d, 2H, $^3J = 8.11$ Hz, CH-arom.), 7.10 (d, 2H, $^3J = 8.11$ Hz, CH-arom.), 2.37 (s, 3H, CH_3), -0.02 (s, 18H, $\text{CH}_3\text{-Si}$).

3.4. Olefin polymerization experiments

These experiments were conducted in a 100-ml flame-dried round-bottomed reaction flask attached to a high-vacuum line. In a typical experiment 6 mg (8.7×10^{-3} mmol) of the catalyst and 200 mg of MAO were placed in a 100 ml flask containing a magnetic stir bar. The reaction vessel was connected to a high-vacuum line, pumped-down and back-filled three times and the flask was then re-evacuated and a measured quantity of toluene (30 ml) was vacuum transferred into the flask over Na–K. Gaseous ethylene was then admitted to the vessel, after temperature equilibration, through the gas purification column. The gas pressure was maintained continuously at 1.0 atm with a mercury manometer. Rapid stirring of the solution was begun and, after a measured time, the polymerization was stopped by injecting methanol–HCl. The polymeric product was filtered off, washed with acetone and pentane and dried under vacuum. Pressurized reactions were performed in a similar fashion in a 500 ml stainless-steel reactor interfaced to a high-vacuum line. The ethylene was condensed into the reactor at low temperature and the vessel was then warmed to room temperature. The quenching and the collection of the product were performed as for the atmospheric pressure reactions.

Acknowledgement

This research was supported by the Israel Science Foundation administered by the Israel Academy of Sciences and Humanities under Contract 76/94-1 and by the Technion V.P.R. Fund. We thank Dr. Enno Lork of the Department of Chemistry at Bremen University for the crystallographic measurements.

References

- [1] For recent reviews on olefin polymerization catalysts, see (a) R.P. Quirk (ed.), *Transition Metal Catalysed Polymerizations*, Cambridge University Press, Cambridge, 1988; (b) W. Kaminsky and H. Sinn (eds.), *Transition Metals and Organometallics for Catalysts for Olefin Polymerization*, Springer, New York, 1988; (c) J.A. Ewen, in T. Keii and K. Soga (eds.), *Catalytic Polymerization of Olefins*, Elsevier, New York, 1986, p. 271; (d) R.F. Jordan, P.K. Bradley, R.E. LaPointe, and D.F. Taylor, *New J. Chem.*, 14 (1990) 499; (e) R.F. Jordan, *Adv. Organomet. Chem.*, 32 (1991) 325.
- [2] For some recent references, see (a) X. Yang, C.L. Stern and T.J. Marks, *J. Am. Chem. Soc.*, 116 (1994) 10015; (b) G. Erker, M. Aulbach, C. Kruger and S. Werner, *J. Organomet. Chem.*, 450 (1993) 1; (c) M. Farina, G. Disilvestro and P. Sozzanin, *Macromolecules*, 26 (1993) 946; (d) W. Kaminsky, A. Bark and R. Steiger, *J. Mol. Catal.*, 74 (1992) 109; (e) J.C.W. Chien, G.H. Llinas, M.D. Rausch, Y.G. Lin, H.H. Winter, J.L. Atwood and S.G. Bott, *J. Polym. Sci., Part A, Poly. Chem.*, 30 (1992) 2601; (f) J. Okuda, *Angew. Chem., Int. Ed. Engl.*, 31 (1992) 47; (g) L. Resconi, L. Abis and G. Francisccono, *Macromolecules*, 25 (1992) 6814; (h) K. Mashima, S. Fujikawa and A. Nakamura, *J. Am. Chem. Soc.*, 115 (1993) 10990; (i) G. Erker, *Pure Appl. Chem.*, 64 (1992) 393; (j) W. Spaleck, M. Antberg, J. Rohrmann, A. Winter, B. Bachmann, P. Kiprof, J. Behm and W.A. Herrmann, *Angew. Chem., Int. Ed. Engl.*, 31 (1992) 1347, and references cited therein.
- [3] See, for example, (a) S. Collins, W.J. Gauthier, D.A. Holden, B.A. Kuntz, N.J. Taylor and D.G. Ward, *Organometallics*, 10 (1991) 2061; (b) W. Roll, H.H. Brintzinger, B. Rieger and R. Zolk, *Angew. Chem., Int. Ed. Engl.*, 29 (1990) 279; (c) I.M. Lee, W.J. Gauthier, J.M. Ball, B. Iyengar and S. Collins, *Organometallics*, 11 (1992) 2115; (d) S.L. Borkowsky, N.C. Baenziger and R.F. Jordan, *Organometallics*, 12 (1993) 486; (e) Y.W. Alelynnas, Z. Guo, R.E. La Pointe and R.F. Jordan, *Organometallics*, 12 (1993) 544; (f) M. Bochmann and S.J. Lancaster, *Organometallics*, 12 (1993) 633; (g) M. Bochmann and A.J. Jaggat, *J. Organomet. Chem.*, 434 (1992) C1.
- [4] (a) D. Fenske, E. Hartmann and K. Dehnicke, *Z. Naturforsch., Teil B*, 43 (1988) 1611; (b) K. Dehnicke, C. Ergezinger, E. Hartmann, A. Zinn and K. Hösler, *J. Organomet. Chem.*, 352 (1988) C1; (c) M. Wedler, F. Knösel, F.T. Edelmann and U. Behrens, *Chem. Ber.*, 125 (1992) 1313; (d) M. Wedler, A. Recknagel, J.W. Gilje, M. Noltemeyer and F.T. Edelmann, *J. Organomet. Chem.*, 426 (1992) 295; (e) F.T. Edelmann, W. Ziegler and U. Behrens, *J. Organomet. Chem.*, 426 (1992) 261, and references cited therein.
- [5] M.S. Eisen and M. Kapon, *J. Chem. Soc., Dalton Trans.*, (1994) 3507.
- [6] H.W. Roesky, B. Meller, M. Noltemeyer, H.-G. Schmidt, U. Scholtz and G.M. Scheldrick, *Chem. Ber.*, 121 (1988) 1403.
- [7] A. Recknagel, F. Knösel, H. Gornitzka, M. Noltemeyer and F.T. Edelmann, *J. Organomet. Chem.*, 417 (1991) 363.

- [8] D.G. Dick, R. Duchateau, J.J.H. Edeme and S. Gambarotta, *Inorg. Chem.*, **32** (1993) 1959.
- [9] M. Wedler, M. Noltmeyer, U. Pieper, H.-G. Schmidt, D. Stalke and F.T. Edelmann, *Angew. Chem., Int. Ed. Engl.*, **29** (1990) 894.
- [10] R. Gómez, M.L.H. Green and J.L. Haggitt, *J. Chem. Soc., Chem. Commun.*, (1994) 2607
- [11] A. Chernega, R. Gómez and M.L.H. Green, *J. Chem. Soc., Chem. Commun.*, (1993) 1415
- [12] I. Cragg-Hine, M.G. Davidson, F.S. Mair, P.R. Raithby and R. Snaith, *J. Chem. Soc., Dalton Trans.*, (1993) 2423.
- [13] J.L. Koenig, *Spectroscopy of Polymers*, American Chemical Society, Washington, DC, 1992, p. 137.
- [14] For a summary on reaction pathways, see (a) H. Sinn and W. Kaminsky, *Adv. Organomet. Chem.*, **18** (1980) 99; (b) M. Bochmann, T. Cuenca and D.T. Hardy, *J. Organomet. Chem.*, **484** (1994) C10.
- [15] M.A. Giardello, M.S. Eisen, C.L. Stern and T.J. Marks, *J. Am. Chem. Soc.*, **115** (1993) 3326, and references cited therein.
- [16] R. Duchateau, C.T. van Wee, A. Meetsma and J.H. Teuben, *J. Am. Chem. Soc.*, **115** (1993) 4931, and references cited therein.
- [17] For some recent references, see: (a) P.J. Shapiro, W.D. Cotter, W.P. Schaefer, J.A. Labinger and J.E. Bercaw, *J. Am. Chem. Soc.*, **116** (1994) 4623; (b) E.P. Bierwagen, J.E. Bercaw and W.A. Goddard, III, *J. Am. Chem. Soc.*, **116** (1994) 1481; (c) H.K. Kuribayashi, N. Koga and K. Morokuma, *J. Am. Chem. Soc.*, **114** (1992) 2359; (d) H.K. Kuribayashi, N. Koga and K. Morokuma, *J. Am. Chem. Soc.*, **114** (1992) 8687.
- [18] For recent theoretical studies on Ziegler–Natta polymerizations, see: (a) L. Resconi, F. Piemontesi, G. Franciscano, L. Abis and T. Fiorani, *J. Am. Chem. Soc.*, **114** (1992) 1025; (b) R.J. Meier, G.H.J. van Doremaele, S. Iarlori and F. Buda, *J. Am. Chem. Soc.*, **116** (1994) 7274; (c) H. Weiss, M. Ehrig and R. Ahlrichs, *J. Am. Chem. Soc.*, **116** (1994) 4919; (d) G. Guerra, L. Cavallo, G. Moscardi, M. Vacatello and P. Corradini, *J. Am. Chem. Soc.*, **116** (1994) 2988; (e) J.R. Hart and A.K. Rappé, *J. Am. Chem. Soc.*, **115** (1993) 6159.